Final Semester Report

Dev Shah

Georgia Institute of Technology

ME 4699 – Undergraduate Research

Faculty Advisor: Dr. M. Ghiaasiaan

Fall 2025

Abstract

This report documents a semester-long effort into understanding the workings of Thermo-Radiative Cell (TR Cell) Technologies. The primary objective was to quantify the radiative power emitted by a 300 K TR cell and heater assembly and to understand how this power affects the temperature of a cold plate thermally linked to a cryocooler with a nominal refrigeration capacity of 1.0 W at 4.2 K. The TR cell and heater were modeled as a blackbody disk with a diameter of one inch, while the receiver was a copper cold plate of diameter 2.52 m. Using the Stefan–Boltzmann law, the radiative heat load from the emitter was estimated and then combined with a thermal resistance model for the conduction path between the cold plate and the cold head. This analysis showed that even modest radiative powers on the order of 0.05 W to 0.2 W can significantly impact the cold-head temperature because of the limited cryocooler capacity. After making initial calculations and understanding the relevant concepts, the second half of the semester was devoted to waiting for the right parts, mounting the CryoCooler and testing the Terranova 934 Vacuum Pump.

To build foundational skills in two and three-dimensional fluid dynamics, I learned how to model the Coanda effect on Ansys fluent after being tasked to create and dimension a double-helical coil geometry from a separate project. This work provided experience in geometry creation, meshing, boundary-layer treatment, and turbulence modeling, which was then leveraged to study a double-helical internal flow geometry representative of a compact heat exchanger.

Finally, my contributions this semester included scientific figure production, the most occupying of which was redrawing a deep learning model diagram using and the 'TikZ'package on LaTex for publication-quality presentation.

Overall, the work developed a quantitative understanding of radiative loading in cryogenic TR-cell systems, practical hands-on experience with cryogenic and vacuum hardware, and improved modeling and documentation skills for complex three-dimensional flow systems.

Contents

1 Introduction and Research Objectives

ThermoRadiative (TR) cells are a class of energy-conversion devices that exploit radiative heat exchange between a warm emitter and a cold reservoir to generate useful work. In TR-cell experiments, the warm emitter (typically near room temperature) radiates toward a cryogenic receiver, often interfaced with a cryocooler operating near the boiling point of liquid helium. Because cryocoolers have strictly limited cooling capacities at low temperature, understanding radiative heat loads is essential for designing viable experiments and prototypes.

The work presented in this report had four major goals:

1. Model the radiative power emitted by a 300 K TR cell and heater assembly approximated as a blackbody disk.

2. Evaluate how this radiative power affects the temperature of a copper cold plate thermally linked to a cryocooler with a capacity of approximately 1 W at 4.2 K.

3. Characterize the influence of the thermal link between the cold plate and the cold head, including the impact of materials (OFHC copper vs. regular copper), screws, and thermal grease.

In addition to analytical modeling, significant time was spent on experimental setup: learning to operate the cryocooler and vacuum system, troubleshooting instrumentation, and preparing the system for future TR-cell measurements.

2 System Description

This section aims to provide a background of all the dimensions of our model and the Heat Transfer Model derived from this.

2.1 TR Cell and Emitter Geometry

The TR cell and heater assembly were modeled as a circular emitting surface:

- Diameter: 1.0
- Radius: $r = 0.5 = 0.0127 meter$

The surface area of the emitter is thus

$$A_{\text{emit}} = \pi r^2 = \pi(0.0127\,\text{m})^2 \approx 5.07 \times 10^{-4}\,\text{m}^2. \tag{1}$$

For the purposes of this study, the emitter was assumed to be a 300 K blackbody or, more realistically, a gray body with emissivity close to unity.

2.2 Cold Plate and Cryocooler

The receiving surface was a circular cold plate mounted to the cold head of a cryocooler:

- Diameter: 2.52
- Material: Oxygen-Free High Conductivity (OFHC) copper or regular copper
- Nominal cold-head temperature: 4.2 K at 1.0 W of cooling capacity

The cryocooler performance curve indicates that the available cooling power decreases rapidly as the desired operating temperature approaches 4 K. Consequently, even small parasitic heat loads can cause a noticeable increase in the cold-head temperature.

3 Radiative Heat Transfer Modeling

3.1 Stefan–Boltzmann Law

The radiative heat flux from a blackbody surface at temperature T is given by the Stefan–Boltzmann law:

$$q = \sigma T^4, \tag{2}$$

where $\sigma = 5.67 \times 10^{-8}\,\mathrm{W\ m^{-2}K^{-4}}$ is the Stefan–Boltzmann constant. For a finite surface area A, the total radiated power is

$$P = A\sigma T^4. \tag{3}$$

For the 300 K TR emitter,

$$q = \sigma T^4 = 5.67 \times 10^{-8}(300\,\mathrm{K})^4 \approx 459\,\mathrm{W\ m^{-2}}, \tag{4}$$

$$P_{\mathrm{BB}} = A_{\mathrm{emit}}\, q \approx \left(5.07 \times 10^{-4}\,\mathrm{m^2}\right)\left(459\,\mathrm{W\ m^{-2}}\right) \approx 0.233\,\mathrm{W}. \tag{5}$$

Thus a small one-inch-diameter emitter at 300 K emits approximately 0.23 W of radiative power if it behaves as an ideal blackbody.

3.2 Gray-Body and View-Factor Corrections

In practice, the TR cell is a gray body with emissivity $\varepsilon < 1$, and only a fraction of the emitted radiation is intercepted by the cold plate. The absorbed power can be estimated as

$$P_{\mathrm{abs}} = \varepsilon A_{\mathrm{emit}} \sigma T^4 F_{12}, \tag{6}$$

where F_{12} is the view factor from the emitter (1) to the receiver (2).

Typical values for this preliminary analysis might be $\varepsilon \approx 0.8$ and $F_{12} \approx 0.3$–0.6, depending on the cavity geometry and any shielding. These values give a range of absorbed

powers,

$$P_{\text{abs}} \approx 0.05\text{–}0.12\,\text{W}, \tag{7}$$

which already represents 5 % to 12 % of the cryocooler capacity at 4.2 K. This illustrates the importance of radiative shielding and careful design of the emitter–receiver geometry.

3.3 Sensitivity to Emitter Temperature

Because radiative power scales as T^4, modest changes in emitter temperature have a large impact on the heat load. For example, if the TR cell operates at 320 K instead of 300 K,

$$\frac{P(320\,\text{K})}{P(300\,\text{K})} = \left(\frac{320}{300}\right)^4 \approx 1.28, \tag{8}$$

so the radiative power increases by about 28 %. Such sensitivity must be accounted for when sizing cryogenic components and predicting steady-state temperatures.

4 Thermal Link and Conduction to the Cold Head

4.1 Thermal Resistance Network

The cold plate is thermally connected to the cryocooler cold head through a mechanical joint involving screws, contact surfaces, and thermal grease. The conductive heat transfer through this joint can be approximated by a thermal resistance network,

$$\dot{Q}_{\text{cond}} = \frac{T_{\text{plate}} - T_{\text{head}}}{R_{\text{th}}}, \tag{9}$$

where:

- T_{plate} is the temperature of the cold plate,
- T_{head} is the temperature of the cryocooler cold head,

- R_{th} is the effective thermal resistance of the link.

The total thermal resistance is the sum of the bulk conduction resistance of the copper elements and the contact resistances at each interface.

4.2 Effect of OFHC Copper

Oxygen-Free High Conductivity copper (OFHC) has very high thermal conductivity at cryogenic temperatures, with values commonly exceeding $400\,\frac{\text{W}}{\text{m K}}$ and reaching significantly higher values below 20 K. Replacing regular copper components with OFHC copper thereby reduces the bulk component of R_{th} and improves the ability of the cold head to sink heat from the plate. However, if contact resistances are large, they may dominate the total thermal resistance, limiting the benefit of improved bulk conductivity.

4.3 Role of Contact Resistance and Thermal Grease

The interfaces between the cold plate, intermediate straps, and cold head often control the overall thermal performance. Microscopic surface roughness reduces the real contact area, introducing substantial thermal resistance. Tightening screws to higher torque increases the real contact area, and applying thermal grease fills microscopic voids, both of which reduce contact resistance. Therefore, careful mechanical assembly and surface preparation are critical for achieving low R_{th} and keeping the cold-head temperature close to the ideal value predicted by the cryocooler performance curve.

5 Vacuum System and Cryocooler Commissioning

In addition to analytical work, a substantial part of the semester was spent learning to operate and troubleshoot the vacuum system and cryocooler used for TR-cell experiments.

5.1 Terranova Vacuum Controller and Pressure Measurement

The vacuum system employs a Terranova controller with ion gauges capable of measuring pressures down to the $10^{-}6torrrange.Duringthesemester, practicalexperiencewasacquiredin$:

Operating the controller and interpreting dual-channel pressure displays.

Managing filament warm-up and avoiding filament burnout.

Recognizing and responding to error codes (e.g., filament failure).

Determining acceptable pressure ranges for cryocooler operation.

Achieving and maintaining high vacuum is essential for minimizing convective heat transfer to the cold components and for ensuring stable cryocooler performance.

5.2 Turbo Pump Operation

The system's high-vacuum stage is supported by a turbo-molecular pump. Experimental tasks included:

- Proper pump startup and shutdown sequences.
- Monitoring backing-pump performance.
- Ensuring that the system is free of leaks that would prevent the turbo from reaching its design speed.

These activities provided hands-on experience with typical issues encountered in vacuum technology.

5.3 Cryocooler Handling and Mounting

The cryocooler cold head must be mechanically integrated with the cold plate and thermal link. During the semester, time was spent:

- Physically mounting and aligning the cryocooler.
- Verifying mechanical stability and thermal contact.
- Observing cooldown curves during test runs.

Although significant time was spent waiting for parts to arrive, the experience built familiarity with the experimental hardware that will be used for future TR-cell measurements.

6 Coandă Effect Modeling as a Pathway to 3D Flow Simulation

6.1 Motivation

Before attempting to model complex three-dimensional flows in double-helical channels, it was necessary to gain experience with computational fluid dynamics in simpler but still physically rich configurations. The Coandă effect—the tendency of a jet to attach to a nearby curved surface—provided an ideal intermediate step. It involves wall curvature, boundary layers, entrainment, and separation phenomena that also play important roles in more advanced geometries.

6.2 Geometry and Boundary Conditions

A two-dimensional curved-wall geometry was constructed to mimic an impinging jet that deflects along a smooth surface. The main features of the model included:

- An inlet jet with specified velocity profile.
- No-slip boundary conditions on the walls.
- A smoothly curved surface designed to generate Coandă attachment.
- A pressure outlet boundary condition downstream.

Several inlet velocities were tested to examine the influence of Reynolds number on the attachment behavior.

6.3 Turbulence Modeling and Mesh Considerations

A shear-stress-transport (SST) k–ω turbulence model was selected because of its robustness for wall-bounded flows with adverse pressure gradients. Mesh refinement studies emphasized the need for adequate resolution near the wall (low y^+) to correctly capture the boundary layer and attachment behavior.

6.4 Results and Interpretation

Figure **??** shows a representative velocity-contour plot from the Coandă simulations. Across the range of inlet velocities considered, the general shape of the pathlines remained similar, with a jet attaching to the curved surface and following it downstream. Higher velocities increased velocity gradients and shear stresses but did not fundamentally alter the attachment behavior, underscoring the geometric nature of the effect over the range studied.

6.5 Preparation for Double-Helical Modeling

The Coandă simulations developed key skills relevant to three-dimensional CFD:

- Creating and modifying geometries with curved boundaries.
- Generating and refining meshes for wall-bounded turbulent flows.
- Selecting turbulence models and interpreting their limitations.
- Checking convergence and validating flow behavior qualitatively.

These experiences laid the groundwork for modeling more complex internal flows in double-helical geometries.

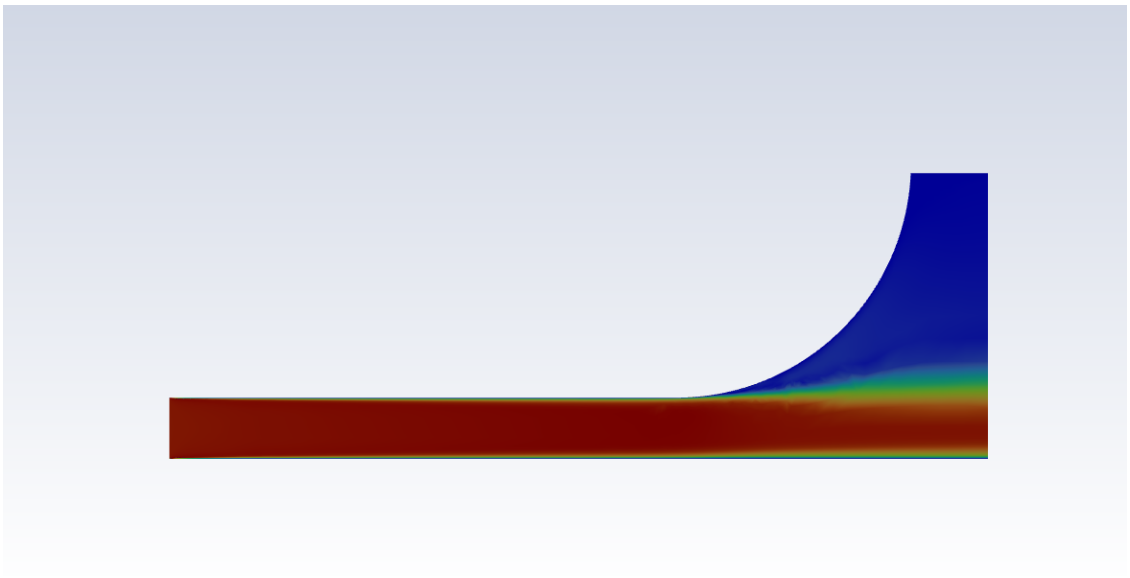

Figure 1: Representative velocity-contour and pathline visualization of the Coandă effect. A jet issuing from the left attaches to a curved wall and follows it, illustrating the role of wall curvature in flow deflection.

belfig:coanda

7 Double-Helical Geometry and Navier–Stokes Analysis

7.1 Geometry Description and Re-dimensionalization

The next step was to examine flow through a double-helical internal channel similar to that used in a compact heat exchanger. A representative geometry is shown in Figures **??** and **??**. The flow passage is formed by a helically wound tube contained within a cylindrical shell, creating a long, curved flow path.

For analysis, the geometry was re-dimensionalized in terms of nondimensional parameters such as:

- The ratio of tube radius to shell radius, r/R.
- The dimensionless pitch, p/D, where p is the helical pitch and D is tube diameter.
- The ratio of characteristic channel height to radius, under the assumption that $h \ll R$

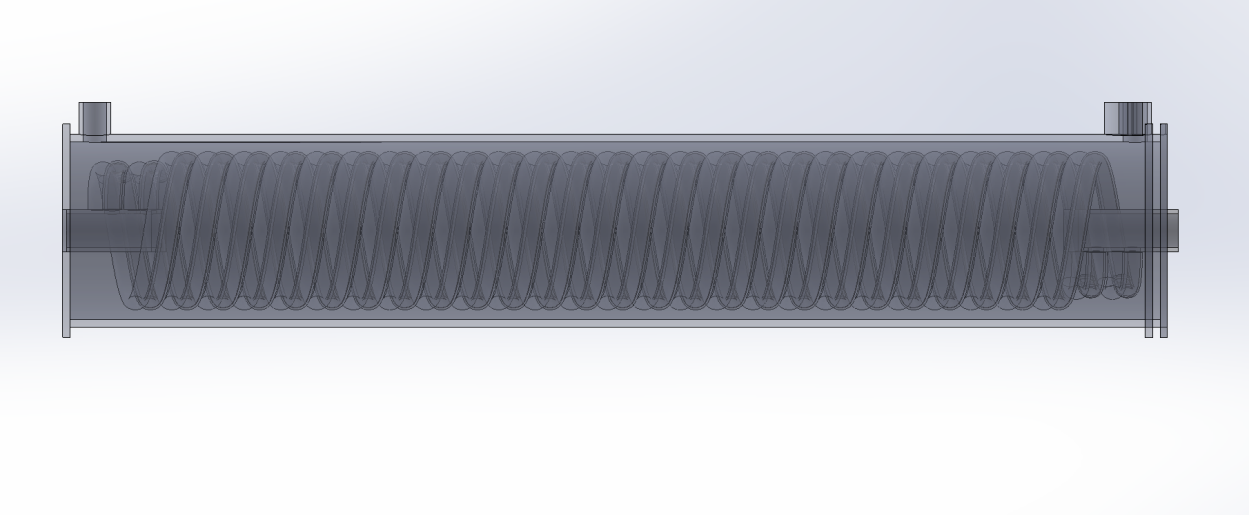

Figure 2: Side view of the double-helical internal geometry within a cylindrical shell. The coils create a long, curved flow path that enhances heat transfer.
belfig:helical$_s ide$

for thin annular gaps.

These nondimensional groups help compare different designs and guide mesh construction for CFD.

7.2 Governing Equations and Simplifications

The incompressible Navier–Stokes equations govern the flow within the helical passages. In a cylindrical coordinate system aligned with the helix, curvature introduces additional terms representing centrifugal forces and pressure gradients in the radial direction. Under certain assumptions, such as small radial velocity components and slender channels, the radial momentum equation simplifies and the pressure variation in the radial direction can be neglected to leading order. This allows one to treat the flow as primarily axial with secondary cross-sectional circulation, which is often studied using Dean-number analysis.

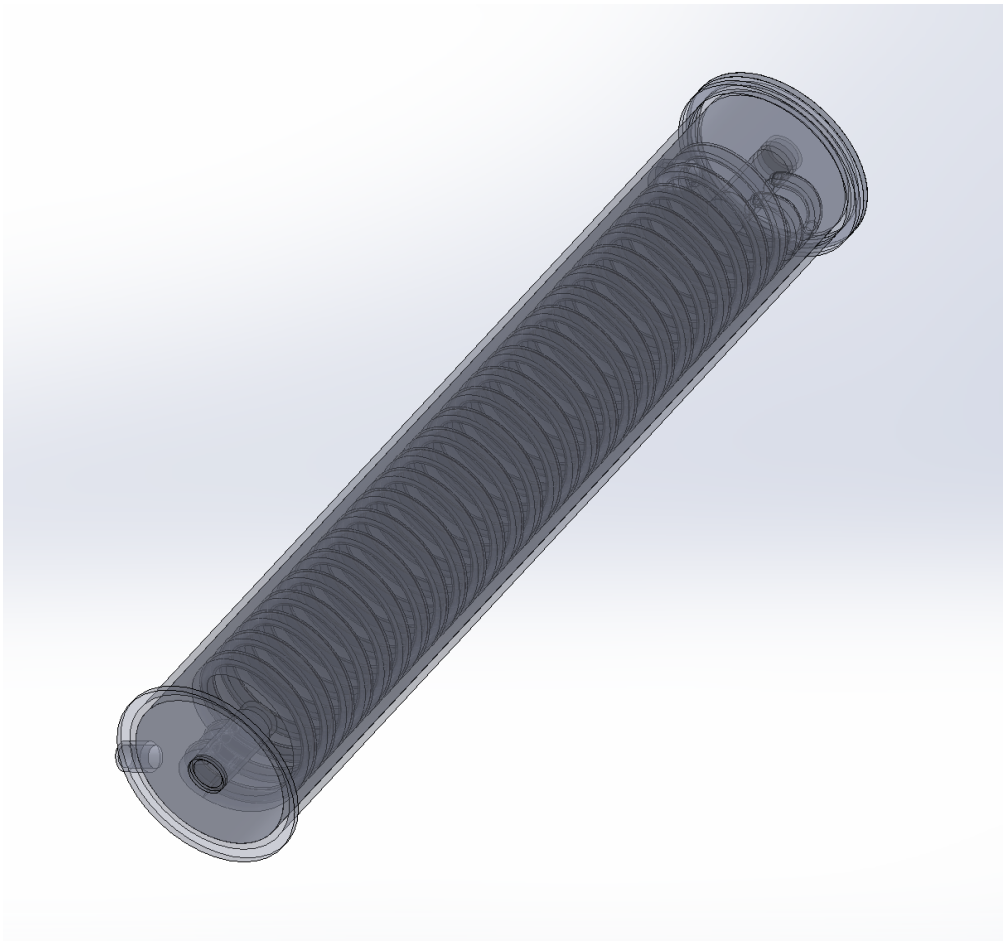

Figure 3: Isometric view of the double-helical assembly. The geometry introduces three-dimensional curvature and secondary flows that complicate the Navier–Stokes analysis.
belfig:helical$_i so$

7.3 Connection to CFD Practice

Although a full CFD solution of the double-helical geometry was beyond the scope of this semester, the preparatory steps included:

- Translating engineering drawings into a clean parametric model.
- Planning mesh strategies for resolving secondary flows.
- Identifying appropriate turbulence models for curved internal flows.

The combination of analytical reasoning and Coandă-based CFD experience provides a strong foundation for future numerical simulations.

8 Machine Learning Model Diagram and TeX Figure Production

8.1 Motivation

An additional component of the semester's work involved scientific communication: producing high-quality diagrams of a deep learning model for use in presentations and publications. This task required learning TeX and TikZ, with emphasis on consistent notation, clear labeling, and aesthetically pleasing layout.

8.2 Final Diagram

The resulting diagram is shown in Figure **??**. It illustrates a feedforward neural network with six inputs, two hidden layers, and two outputs, with full connectivity between successive layers and clearly labeled input and output variables. Bias nodes, weights, and layer boundaries were carefully arranged to avoid clutter and to conform to scientific typesetting conventions.

8.3 Skills Developed

Through this work, the following skills were developed:

- Use of TeX for document preparation, including equation formatting and cross-referencing.
- Creation of vector graphics with TikZ, enabling resolution-independent figures.
- Application of scientific typesetting standards to axes labels, subscripts, and units.

These skills are directly applicable to future research reports, journal submissions, and technical presentations.

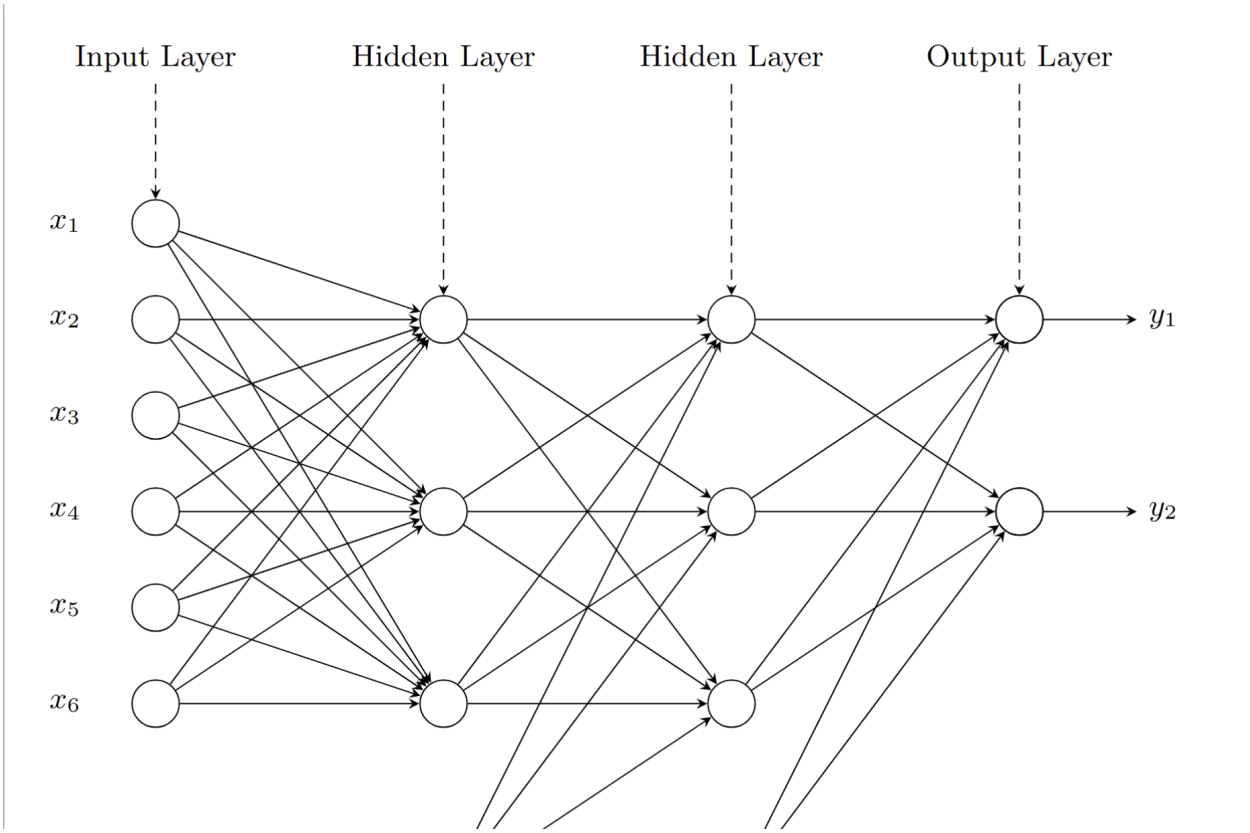

Figure 4: Final deep learning model diagram produced in TeX using TikZ. The figure demonstrates consistent notation, fully connected layers, and clear labeling of inputs and outputs. belfig:nn

9 Conclusions and Future Work

This semester's research combined analytical modeling, experimental preparation, and computational groundwork to build a coherent understanding of ThermoRadiative cell systems and complex internal flows.

On the thermal side, the Stefan–Boltzmann analysis showed that a one-inch-diameter emitter at 300 K emits roughly 0.23 W as a blackbody, and that realistic gray-body and view-factor corrections still produce absorbed powers on the order of 0.05 W to 0.12 W. Given the cryocooler's capacity of 1.0 W at 4.2 K, such radiative loads are non-negligible and must be carefully managed. The importance of thermal-link design, including the choice of OFHC copper and mitigation of contact resistance with screws and thermal grease, was highlighted through a simple thermal-resistance model.

Experimentally, the work provided practical experience with vacuum technology, turbo pumps, and cryocooler mounting, setting the stage for future TR-cell measurements. The commissioning process also revealed the importance of robust instrumentation and the challenges associated with maintaining high vacuum.

On the fluid-mechanics side, modeling the Coandă effect served as an effective gateway to more complex three-dimensional simulations. The Coandă studies developed competence in geometry creation, meshing, turbulence modeling, and qualitative interpretation of CFD results, which are essential skills for studying double-helical flow passages. Preliminary work on the double-helical geometry established a parametric description and identified key nondimensional parameters relevant to future simulations.

Finally, the production of a deep learning model diagram using LaTex and TikZ improved scientific communication skills and led to publication-quality figures for ongoing research projects.

Future work will include:

- Implementing full CFD simulations of the double-helical geometry with realistic boundary conditions.
- Incorporating detailed radiative view-factor computations in the TR-cell model.
- Performing experimental measurements of cold-head temperature under controlled radiative loads to validate the modeling.
- Extending the figure-production workflow to other aspects of the TR-cell and flow-geometry studies.